

Dynamical thermalization of disordered nonlinear lattices

Mario Mulansky,¹ Karsten Ahnert,¹ Arkady Pikovsky,^{1,2} and Dima L. Shepelyansky^{2,3}

¹*Department of Physics and Astronomy, Potsdam University, Karl-Liebknecht-Straße 24, D-14476 Potsdam-Golm, Germany*

²*Laboratoire de Physique Théorique (IRSAMC), Université de Toulouse–UPS, F-31062 Toulouse, France*

³*LPT (IRSAMC), CNRS, F-31062 Toulouse, France*

(Received 12 March 2009; revised manuscript received 2 October 2009; published 24 November 2009)

We study numerically how the energy spreads over a finite disordered nonlinear one-dimensional lattice, where all linear modes are exponentially localized by disorder. We establish emergence of dynamical thermalization characterized as an ergodic chaotic dynamical state with a Gibbs distribution over the modes. Our results show that the fraction of thermalizing modes is finite and grows with the nonlinearity strength.

DOI: [10.1103/PhysRevE.80.056212](https://doi.org/10.1103/PhysRevE.80.056212)

PACS number(s): 05.45.–a, 63.50.–x, 63.70.+h

The studies of ergodicity and dynamical thermalization in *regular* nonlinear lattices have a long history initiated by the Fermi-Pasta-Ulam problem [1] but they are still far from being complete (see, e.g., [2] for thermal transport in nonlinear chains and [3] for thermalization in a Bose-Hubbard model). In this paper, we study how the dynamical thermalization appears in nonlinear *disordered* chains where all linear modes are exponentially localized. Such modes appear due to the Anderson localization introduced in the context of electron transport in disordered solids [4–6] and describing various physical situations such as wave propagation in a random medium [7], localization of a Bose-Einstein condensate [8], and quantum chaos [9].

Effects of nonlinearity on localization properties have attracted large interest recently. Indeed, nonlinearity naturally appears for localization of a Bose-Einstein condensate, as its evolution is described by the nonlinear Gross-Pitaevskii equation [10]. An interplay of disorder, localization, and nonlinearity is also important in other physical systems such as wave propagation in nonlinear disordered media [11,12] and chains of nonlinear oscillators with randomly distributed frequencies [13].

The main question here is whether the localization is destroyed by nonlinearity. It has been addressed recently using two physical setups. In Refs. [14,15] it was demonstrated that an initially concentrated wave packet spreads apparently indefinitely, although subdiffusively, in a disordered nonlinear lattice. For a transmission through a nonlinear disordered layer [16,17], chaotic destruction of localization leads to a drastically enhanced transparency.

Here we study the thermalization properties of the dynamics of a nonlinear disordered lattice—discrete Anderson nonlinear Schrödinger equation (DANSE). We describe in details the features of the time evolution of an initially localized excitation toward a statistical equilibrium in a finite lattice. (We stress that this evolution is purely deterministic and that the relaxation to equilibrium is due to deterministic chaos.) Below we argue that a statistically stationary state is characterized by the Gibbs energy equipartition across the linear eigenmodes [Eq. (5)] and call a relaxation to such an equilibrium state thermalization. Because thermalization is due to deterministic chaos, its rate heavily depends on the statistical properties of the chaos. As is typical for nonlinear Hamiltonian systems, depending on initial conditions one can obtain solutions belonging to a “chaotic sea” or to “regu-

lar islands.” Moreover, one can expect the former to thermalize while the latter do not lead to thermalization. We numerically find nonthermalizing modes and characterize their dependence on the nonlinearity and the lattice length. We stress here that our analysis heavily relies on numerical simulations as analytic methods appear to be hardly applicable for disordered nonlinear systems. In numerics, a difference between thermalizing and nonthermalizing states (as well as between chaotic and nonchaotic states) is limited by the maximal integration time: it might happen that the states which do not thermalize up to some time will thermalize in the future. There is no way to overcome this limitation in a simple way because of a possibility for slow processes such as Arnold diffusion, characteristic time of which lies far beyond any computationally accessibility. Nevertheless, performing an analysis based on large but finite time scales, we can, on one hand, make predictions for experiments, and on the other hand, obtain a “coarse-grained” description of the dynamics. Accordingly, the results below should be understood as valid for available integration times, without a straightforward extrapolation for asymptotically large times.

We describe a nonlinear disordered medium by the DANSE model:

$$i \frac{\partial \psi_n}{\partial t} = E_n \psi_n + \beta |\psi_n|^2 \psi_n + \psi_{n+1} + \psi_{n-1}, \quad (1)$$

where β characterizes nonlinearity and the on-site energies E_n (or frequencies) are independent random variables distributed uniformly in the range $-W/2 < E_n < W/2$ (they are shifted in such a way that $E=0$ corresponds to the central energy of the band). We consider a finite lattice $1 \leq n \leq N$ with periodic boundary conditions. Then DANSE is a classical dynamical system with the Hamilton function

$$H = \sum_n E_n |\psi_n|^2 + \psi_{n-1} \psi_n^* + \psi_{n-1}^* \psi_n + \frac{\beta}{2} |\psi_n|^4. \quad (2)$$

It describes recent experiments with nonlinear photonic lattices (cf. Eq. (1) in [12]), where one follows, along a transversally disordered finite nonlinear crystal, the evolution of a single-site or a single-mode initial state. This corresponds to the setup of our thermalization problem. Thus, the properties below can be observed experimentally as “thermalization of photons” provided the crystal is long enough. In the context

of many-particle quantum systems, Eq. (2) is used as an effective mean-field Hamiltonian of interacting bosons.

For $\beta=0$ all eigenstates are exponentially localized with the localization length $l \approx 96W^{-2}$ (for weak disorder) at the center of the energy band [6]. Below we mainly focus on the case of moderate disorder $W=4$, for which $l \sim 6$ at the center of the band and $l \approx 2.5$ at $E = \pm 2$. For each particular realization of disorder a set of eigenenergies ϵ_m and of corresponding eigenmodes φ_{nm} can be found. In this eigenmode representation $\psi_n = \sum C_m \varphi_{nm}$ the Hamiltonian reads

$$H = \sum_m \epsilon_m |C_m|^2 + \beta \sum_{knji} V_{knji} C_k C_n C_j^* C_i^*, \quad (3)$$

with $\sum_m |C_m|^2 = 1$ and $V_{mm'm_1m'_1} \sim l^{-3/2}$ are the transition matrix elements [18]. This representation is mostly suitable to characterize the spreading of the field over the lattice, since in this basis the transitions take place only due to nonlinearity. Also, the nonlinear correction to the energy is small ($\sim \beta/l$) for one excited mode.

To study the dynamical thermalization in a lattice, we performed direct numerical simulation of DANSE (1) using mainly two methods: the unitary Crank-Nicholson operator splitting scheme with step $\Delta t = 0.1$ as described in [15] and an eighth-order Runge-Kutta integration with step $\Delta t = 0.02$; in both cases the total energy and the normalization have been preserved with high accuracy and both integration schemes gave similar results for all lattice lengths N used. Such a restriction of the accuracy check to the conserved quantities is suitable for chaotic systems. A comparison with other numerical methods for DANSE [19] goes beyond the scope of this paper and will be performed in a longer publication. We started with two types of localized initial states: (A) one site seeded, i.e., $|\psi_n(0)|^2 = \delta_{n,j}$ and (B) one mode initially excited, i.e., $|C_m(0)|^2 = \delta_{m,k}$. For different realizations of disorder, we seeded different possible sites/modes and followed the evolution of the field solving Eq. (1) up to times (in selected runs) $\sim 10^8$. The level of spreading is characterized by the entropy of the mode distribution,

$$S = - \sum \rho_m \ln \rho_m, \quad \rho_m = \overline{|C_m|^2}, \quad (4)$$

where overline means time averaging. For one excited mode $S=0$ while $S=\ln N$ for a uniform distribution over all modes in a lattice of length N . To give an impression of a time evolution of the thermalization process we show in Fig. 1 several representative time dependencies of entropy (4). One can see that for the setup (B) some modes remain localized during the complete integration time (cf. [20]), while others after some transient time evolve to a state with large entropy. For setup (A), the entropy grows in all cases with a tendency to saturation—some states seem to saturate at about $S \approx \ln N$, while others remain at values definitely smaller than $\ln N$ up to the maximal integration time. Especially the results from (B) indicate a strong energy dependence of the spreading behavior, which is studied in this work. In our discussion below we focus therefore on the setup (B) as the mostly nontrivial one.

To derive an approximate expression for the statistically stationary distribution ρ_m , we mention that it should satisfy

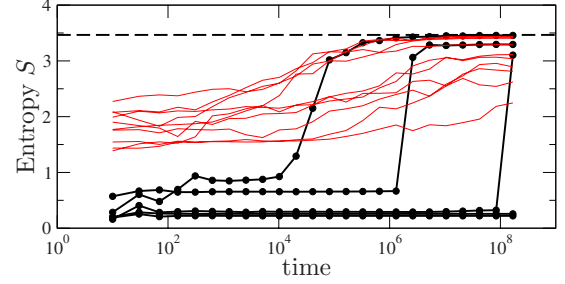


FIG. 1. (Color online) Time evolution of entropy S [Eq. (4)] in DANSE (1) with $N=32$ and $\beta=1$ for a particular realization of disorder and different initial states: bold black curves with markers—single-mode initial states (B) with energies $E = -0.34, 0.76, -0.29, 3.36, -0.5$ (curves from top to bottom at $t = 10^8$, two bottom cases are very close), solid red/gray curves—single-site initial states (A; ten randomly chosen states). The dashed line shows the level $S = \ln 32$. The time averaging has been performed over doubling time intervals (between successive markers).

$\sum \rho_m = 1$ and $E = \sum \rho_m \epsilon_m$, where, in view of the discussion above, we have neglected the nonlinear contribution to the energy. Then the condition of maximal entropy (4) leads, after a standard calculation, to a Gibbs distribution:

$$\rho_m = Z^{-1} \exp(-\epsilon_m/T), \quad Z = \sum_m \exp(-\epsilon_m/T). \quad (5)$$

Here T is an effective “temperature” of the system: it has no meaning as a physical temperature but serves as a parameter characterizing the distribution; it is a function of the total energy E of the state and of the realization of disorder. The entropy and the energy are related to each other via usual expressions, e.g., [21]:

$$E = T^2 \partial \ln Z / \partial T, \quad S = E/T + \ln Z. \quad (6)$$

This value of entropy yields the maximal possible equipartition for the given initial energy, and the values of Fig. 1 obtained via a numerical simulation of the disordered nonlinear lattice should be compared with these values from the Gibbs distribution. Because we have anyhow neglected the effects of nonlinearity in the theoretical value of the entropy, we adopt other simplifications: approximate the density of states of the disordered system as a constant in an interval $-\Delta < \epsilon < \Delta$ and consider the energy eigenvalues ϵ_m in a particular realization of disorder as independent random variables distributed according to this density. Furthermore, we assume the variations of the partition sum to be small and use $\langle \ln Z \rangle \approx \ln \langle Z \rangle$, where brackets denote averaging over disorder realizations. In this simplest approximation we obtain

$$\langle \ln Z \rangle \approx \ln N + \ln \sinh(\Delta/T) - \ln(\Delta/T). \quad (7)$$

At $W=4$ we have $\Delta \approx 3$ (see Figs. 3 and 4 below) and this theory gives the dependence $S(E)$ within a few percent accuracy compared to S averaged over disorder within Gibbs computations with exact numerical values ϵ_m . This justifies, for the parameters used, the approximation above. We note that $T = +0, \pm \infty, -0$ correspond to $E = -\Delta, 0, +\Delta$, respectively (as in the standard two-level problem, see related discussion in [21]).

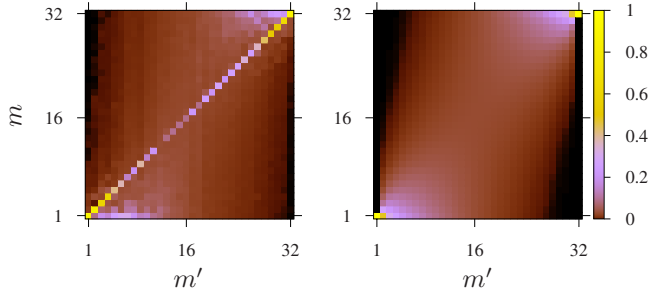


FIG. 2. (Color online) Left: time and disorder averaged probability $\langle \rho_m(m') \rangle$ in mode m for initial state in mode m' . Right: theoretical values according to Gibbs distribution (5). Here $N = 32$, $\beta = 1$, $N_d = 15$.

We compare in Fig. 2 Gibbs distribution (5) with the results of direct numerical simulations of DANSE using N_d disorder realizations. Here we present the values $\langle \rho_m \rangle$ averaged over time and over different realization of disorder in dependence of the number of the initially seeded mode m' . The modes have been ordered according to their energy, so that $m=1$ corresponds to the maximal energy. One can see a good correspondence between the numerics and the simple theory (5) in the sense that states at the band edges remain localized, while states in the center generally spread. However, there is one crucial discrepancy: the peaks on the diagonal $m=m'$ indicate that there are cases when there is no thermalization within our simulation time and the energy remains in the initially seeded mode.

To characterize thermalized and nonthermalized cases quantitatively, we compare in Fig. 3 numerical values for $S(E)$ according to Eq. (4) with the theoretical Gibbs computation given by Eqs. (5)–(7). Clearly, the Gibbs theory gives a satisfactory global description of numerical data. The nonthermalized modes in this presentation are those at the bottom of the graph; these states are absent for the setup (A) where initial sites are seeded. (Again, as discussed above, “nonthermalized” should be understood as “nonthermalized within the integration time.”)

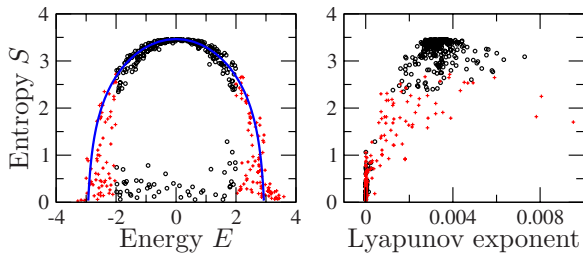


FIG. 3. (Color online) Left panel: final entropies (4) after an evolution during time interval 10^7 averaged over a time interval of 10^6 . The states evolving from initial modes in the middle of the band (see text) are marked with black circles, while those at the edges of the band are marked by the red (gray) pluses. The curve shows approximate theory (7). Right panel: Lyapunov exponents (averaged over a time interval 10^6) vs entropy for the same sets with the same markers. Here $N=32$, $\beta=1$, $N_d=7$. Note that the states with $S \leq 1$ and $-2 \leq E \leq 2$ have nearly zero Lyapunov exponent (although hardly visible in the right panel because overlapped by the red/gray pluses).

It appears appropriate to discuss the dynamics of the modes in the middle of the energy band ($|\epsilon_m| < 2$) and at the edges ($|\epsilon_m| > 2$) separately. For the modes in the middle of the band, the maximal entropy according to Eq. (6) is close to $\ln N$, and one clearly distinguishes the thermalized modes and those that remain localized, as those reaching the maximal entropy and those remaining at the level $S \leq 1$, correspondingly. Thermalization is associated with the chaotic dynamics of the DANSE lattice. To demonstrate this, we calculated the largest Lyapunov exponents λ shown in Fig. 3 (right panel). All modes with $S < 1$, i.e., those that do not thermalize, have nearly vanishing λ , while for the thermalized states ($S > 2$) the positive values of λ clearly indicate chaos.

The above distinction between thermalized and nonthermalized states is less evident for modes at the band edges (shown by red(gray) pluses in Fig. 3). Here already the theoretical value of entropy given by Eqs. (5)–(7) is rather small. Hence, the spreading can go over a few “available” modes only. Nevertheless, also here one can see from Fig. 3 a clear correlation between the entropy and the Lyapunov exponent. Moreover, in several cases the Lyapunov exponent at the edge of the spectrum is definitely larger than in the middle. This happens because the energy spreads over a small number of modes; hence, the effective nonlinearity is larger due to larger amplitudes of each mode, and therefore chaos is stronger.

Above, we did not account for a spatial organization of the mode structure. The latter is less important for the modes in the middle of the band, where one can always expect to find neighbors with a close energy. Contrary to this, for the energies at the edges the issue of spatial distance becomes essential. Indeed, since here the thermalization is possible only over a few modes, it is important whether these modes are spatially separated or not. For linear eigenmodes m and m' the natural measure of this separation is the coupling matrix element $V_{m'm'm}$ according to Eq. (3). It is exponentially small for spatially separated modes due to their localization. One can expect that a mode at the edge of the spectrum will be thermalized only if the coupling V to other few modes in the lattice with a close energy is large, which is a rather rare event.

Finally, we discuss how the thermalization properties depend on the nonlinearity constant β . In Fig. 4 we show the dependence $S(E)$ for different nonlinearities β . For $\beta=0.5$ a large portion of the initial states remains nonthermalized, while for $\beta=2$ all states are thermalized (at least in the sense that their entropy is close to the maximal possible one; as discussed above this is a good criterion in the middle of the band). To determine how the fraction of thermalized states depends on nonlinearity β we use the following procedure. For the initial modes in the middle of the band (i.e., for $|E| < 2$) we classified those that reach more than the half of the maximal entropy [i.e., the level $\ln(N)/2$] as thermalized and those that remain below this level as nonthermalized. The fraction f_{th} of the thermalized modes, shown in Fig. 5, monotonously increases with β . At fixed β the numerical data indicate saturation of f_{th} at large N , but more detailed checks at larger sizes and longer times are required. For example, recent results on self-induced transparency of a disordered

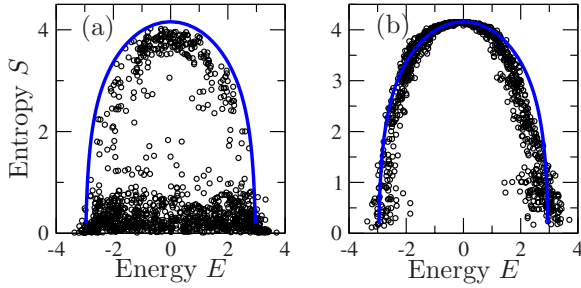


FIG. 4. (Color online) Dependence of entropy S on energy E as in Fig. 2 but for $N=64$, $N_d=18$, and two values of nonlinearity: (a) $\beta=0.5$; (b) $\beta=2$. Averaging has been performed over the time interval 10^6 after an initial evolution during time 10^6 ; for small β still longer times are needed to reach thermalized state with maximal S at given E . The curves are the same theoretical estimates as in Fig. 3.

nonlinear layer [17] show decrease in critical β with lattice size for $N \leq 32$.

The properties of thermalization described above can be incorporated in a general framework of nonlinear dynamics as follows. One can expect, based on general Kolmogorov-Arnold-Moser arguments, that for small nonlinearity regular nonergodic regimes predominate, while for large values of β stable solutions are destroyed and a chaotic ergodic state establishes in the lattice. While it is hard to characterize this transition via a general analysis of the dynamics in a high-dimensional phase space, it is possible to follow the evolution, as nonlinearity increases, of special resonant modes that stem from linear ones. Looking for solutions of Eq. (1) in the form $\psi_n(t) = \phi_n e^{-i\epsilon t}$, we arrive at a nonlinear eigenvalue problem $\epsilon \phi_n = E_n \phi_n + \beta \phi_n^3 + \phi_{n-1} + \phi_{n+1}$ which, of course, at $\beta=0$ yields linear frequencies and modes. Starting from these modes, we followed these solutions to larger nonlinearities using a numerical continuation and in this way obtained nonlinear resonant modes—“breathers” (cf. [20,22]). Worth noting, these modes change in the regions where the field is large, while in the tails they follow linear solutions in accordance with [23]. Moreover, we performed numerical stability analysis of these breathers and found that they bifurcate at some critical value of nonlinearity β_c . The values of β_c for an ensemble of realizations of random potentials are shown in Fig. 5(b). Additionally, we show in Fig. 5(a) a cumulative distribution of β_c for the same range of eigenenergies $|\epsilon_n| < 2$ that is used for the other curves plotted. First of all, note the similar global behavior of f_{th} and f_b which makes us believe that the bifurcations of stable resonant modes are indeed the mechanism of the β dependence of thermalization. However, the curves do not coincide because β_c is defined as the value of the first bifurcation, which may not immediately lead to chaos but may be the first one in a series of transitions to more irregularity. Strictly speaking, f_b should be an upper bound for f_{th} , which is seen in Fig. 5(a). The increase in f_{th} from $t=10^6$ to 10^7 shows that it has not saturated yet, but the saturation curve must lie below f_b .

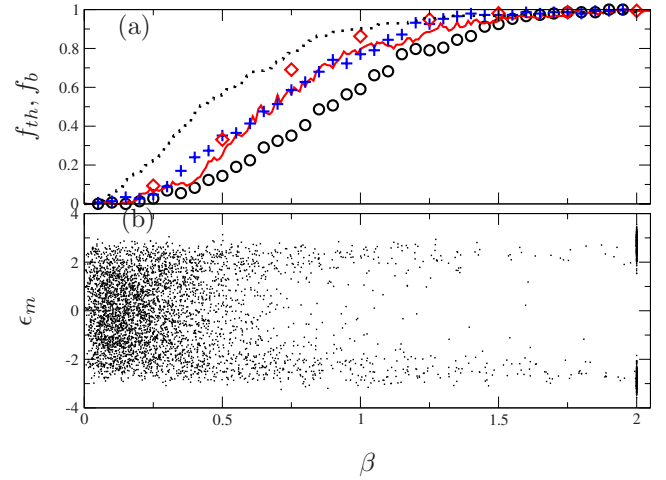


FIG. 5. (Color online) (a) Fraction of thermalized (after time 10^6) modes f_{th} from the middle of the band as a function of nonlinearity β for $N=16$ (circles), 32 (bold line), and 64 (pluses). Diamonds show data for $t=10^7$ and $N=32$. The dotted line shows the fraction of the bifurcated breathers f_b according to panel (b). Panel (b): the bifurcation values β_c for different modes vs their linear energies ϵ_m for $N=32$. To all modes with $\beta_c > 2$ we have attributed $\beta_c=2$; this set looks like two vertical “lines” at $\beta=2$ on panel (b).

Remarkably, we have found that the breathers at the edges of the band, i.e., for $|\epsilon_n| > 2$, are extremely stable: most of them remain stable up to large values of $\beta \approx 5$. This corresponds to the numerical observation of the strong suppression of the thermalization for these modes. We emphasize here that because of the nonlinearity of the system the superposition principle does not hold. This means that to observe a stable breather mode one has to prepare initial conditions mostly close to this solution—which is achieved here by choosing the initial conditions as a pure linear eigenmode (case B above). When one initially seeds one site, as in case A (or uses other initial conditions not close to a breather), then this initial condition does not produce a breather because the latter typically does not survive nonlinear interaction with other components of the solution. If, for example, one starts with an excitation of two modes which are both stable at some value of β , one might still see fast thermalization because a superposition of two breathers is not a breather.

Our main conclusion is that the maximally thermalized state in a disordered nonlinear lattice [Eq. (1)], which emerges as a result of chaotic dynamics, is described by the Gibbs distribution over the linear modes, with some effective *temperature* depending on the initial excitation. Not all modes lead to thermalization; some fraction of them remains localized, but this fraction decreases with nonlinearity. We found that this can be explained by the disappearance (via bifurcations) as the nonlinearity increases of stable resonant modes—breathers—stemming from linear eigenstates. Further studies are still required to establish the properties of this thermalization in dependence on the nonlinearity strength, disorder, and lattice size.

- [1] E. Fermi, J. Pasta, S. Ulam, and M. Tsingou, Los Alamos Report No. LA-1940, 1955 (unpublished); E. Fermi, *Collected Papers* (University of Chicago Press, Chicago, 1965), Vol. 2, p. 978.
- [2] S. Lepri, R. Livi, and A. Politi, *Phys. Rep.* **377**, 1 (2003).
- [3] A. C. Cassidy, D. Mason, V. Dunjko, and M. Olshanii, *Phys. Rev. Lett.* **102**, 025302 (2009).
- [4] P. W. Anderson, *Phys. Rev.* **109**, 1492 (1958).
- [5] P. A. Lee and T. V. Ramakrishnan, *Rev. Mod. Phys.* **57**, 287 (1985); I. M. Lifshits, S. A. Gredeskul, and L. A. Pastur, *Introduction to the Theory of Disordered Systems* (Wiley & Sons, New York, 1988).
- [6] B. Kramer and A. MacKinnon, *Rep. Prog. Phys.* **56**, 1469 (1993).
- [7] P. Sheng, *Introduction to Wave Scattering, Localization and Mesoscopic Phenomena* (Springer, Berlin, 2006).
- [8] J. Billy *et al.*, *Nature* (London) **453**, 891 (2008).
- [9] S. Fishman, D. R. Grempel, and R. E. Prange, *Phys. Rev. A* **36**, 289 (1987); B. V. Chirikov, F. M. Izrailev, and D. L. Shepelyansky, *Physica D* **33**, 77 (1988).
- [10] F. Dalfovo *et al.*, *Rev. Mod. Phys.* **71**, 463 (1999).
- [11] S. E. Skipetrov and R. Maynard, *Phys. Rev. Lett.* **85**, 736 (2000); T. Schwartz *et al.*, *Nature* (London) **446**, 52 (2007).
- [12] Y. Lahini, A. Avidan, F. Pozzi, M. Sorel, R. Morandotti, D. N. Christodoulides, and Y. Silberberg, *Phys. Rev. Lett.* **100**, 013906 (2008).
- [13] A. Dhar and J. L. Lebowitz, *Phys. Rev. Lett.* **100**, 134301 (2008); G. S. Zavg, M. Wagner, and A. Lütze, *Phys. Rev. E* **47**, 4108 (1993).
- [14] M. I. Molina, *Phys. Rev. B* **58**, 12547 (1998); G. Kopidakis *et al.*, *Phys. Rev. Lett.* **100**, 084103 (2008); S. Flach, D. O. Krimer, and Ch. Skokos, *ibid.* **102**, 024101 (2009).
- [15] A. S. Pikovsky and D. L. Shepelyansky, *Phys. Rev. Lett.* **100**, 094101 (2008).
- [16] T. Paul, P. Leboeuf, N. Pavloff, K. Richter, and P. Schlagheck, *Phys. Rev. A* **72**, 063621 (2005).
- [17] S. Tietsche and A. S. Pikovsky, *Europhys. Lett.* **84**, 10006 (2008).
- [18] A similar eigenmode representation has a nonlinear kicked quantum rotator model introduced in D. L. Shepelyansky, *Phys. Rev. Lett.* **70**, 1787 (1993).
- [19] P. Castiglione, G. Jona-Lasinio, and C. Presilla, *J. Phys. A* **29**, 6169 (1996).
- [20] G. Kopidakis and S. Aubry, *Phys. Rev. Lett.* **84**, 3236 (2000); *Physica D* **130**, 155 (1999); **139**, 247 (2000).
- [21] L. D. Landau and E. M. Lifshits, *Statistical Mechanics* (Nauka, Moscow, 1976).
- [22] M. V. Ivanchenko, *Phys. Rev. Lett.* **102**, 175507 (2009).
- [23] A. Iomin and S. Fishman, *Phys. Rev. E* **76**, 056607 (2007).